Computer Assisted Mechanics and Engineering Sciences, 7: 449–460, 2000.

Sensitivity analysis of transient metal forming with incompressible linear elements

Horacio J. Antúnez
Institute of Fundamental Technological Research, Polish Academy of Sciences, ul. Świetokrzyska 21, 00-049 Warsaw, Poland

(Received November 3, 1999)

On the basis of a recently developed method which allows the use of linear elements for metal forming simulation within the flow approach, sensitivity analysis is carried out. Aiming at large, industrial problems, attention is focused on the explicit version, which is considered more effective for such problems, although implicit time integration is possible as well. By time step splitting a stabilization sub-matrix is obtained, which allows the use of equal interpolation for velocity and pressure. Specifically, linear triangles and tetrahedra have been used, which are easily generated by automatic meshers. Sensitivity analysis is carried out by the Direct Differentiation Method, with which similar analyses have been performed by the author for the flow approach within a direct solution scheme.

Keywords: sensitivity analysis, metal forming, explicit time integration, split algorithm, flow approach

1. Introduction

An essential feature of numerical simulation of industrial metal forming processes is, among others, the large size of the problem. The problem discretization must be refined enough in order to model complex geometries and to obtain the solution within a satisfactory accuracy. For this reason, in spite of the ever-growing computational capacity, attention is focussed to find more effective methods for numerical simulations. One of the choices that proves to be preferred by researches and engineers in a number of situations are the explicit methods, which do not require the solution of the system matrix. The conditional stability arising in these methods limits the allowed step size, unlike in implicit ones. However in practice the critical value of the time step is frequently of the same order of the time step required for accuracy of the time integration. Therefore the explicit methods definitely become competitive with respect to the implicit ones.

Secondly, in both implicit and explicit methods, by time step splitting, some positive effects, in comparison with the non-fractional-step solution, may be obtained [5, 6]. In particular, a stabilizing sub-matrix is obtained upon discretization of problems holding incompressibility [8, 10]. This property, initially applied in simulation of Newtonian fluids, was recently applied also to metal forming within the flow approach [1, 4, 12]. This fact is said to circumvent the Babuska–Brezzi (BB) condition, which means that arbitrary approximations may be used for both discretized variables — velocity and pressure. Obviously, the simplest choice is to use equal order interpolation for both of them, which is not possible when the BB condition must be satisfied. In particular, linear triangles are attractive for their easy implementation and automatic generation.

The previous discussion justifies the use of an explicit method with time splitting and linear triangles in the framework of the flow approach for metal forming simulation. Further, sensitivity analysis adds important information about the process itself and about numerical features of the method: how do changes in the particular parameters defining both of them affect the solution. The interesting aspect of so-called analytical methods for sensitivity analysis is that they yield such valuable information at a residual cost, once the analysis problem has been solved. As is well known,

to assess their effectiveness, they should be compared with the cost of obtaining the same information by another method, typically by solving twice the perturbed problem and calculating the sensitivity coefficients as numerical derivatives, sometimes called the finite difference approach to sensitivity (FDM). In the case of direct solution methods, the performance of analytical sensitivity analysis is beyond discussion. (A survey of applications to metal forming can be found in [9] including some of the authors' previous work on the subject.) However, in explicit methods, since no inversion of the system matrix is involved, the expected gain of using analytical methods will be less spectacular, although it will still be much more convenient than using the finite difference method.

In this paper the Direct Differentiation Method (DDM) is used to obtain the parameter sensitivity expression corresponding to the model for metal forming simulation in terms of the flow approach with explicit time integration and time step splitting. The sensitivity coefficients are obtained also in two sub-steps but independently of the solution which is being calculated at each sub-step, hence there are no additional time steps for the sensitivity stage. As numerical illustrations of the method, a steady state extrusion process is obtained as the result of a pseudo-transient evolution. Afterwards, upsetting is presented to show the full transient solution. In each case sensitivity results with respect to chosen design parameters are given.

2. Split-based explicit version of the flow approach

According to the flow approach [11] the metal under forming conditions is considered as a non-Newtonian fluid, whose viscosity is a function — among others — of the strain rate tensor. Since dynamic or convective effects can be neglected, the problem is equivalent to that of solving a non-linear and incompressible Stokes problem. For transient problems within an explicit integration scheme the problem has to be posed as allowing some compressibility, and later the amount of it can be set as to be negligible.

The momentum and mass conservation equations read

$$\begin{aligned} \frac{\partial(\rho v_i)}{\partial t} &= \frac{\partial s_{ij}}{\partial x_j} - \frac{\partial p}{\partial x_i} - g_i \,, \\ \frac{\partial \rho}{\partial t} &= -\frac{\partial(\rho v_i)}{\partial x_i} \,, \end{aligned} \tag{1}$$

where v_i is the velocity, s_{ij} the deviator stress tensor, p the pressure, g_i the body force and ρ the material density. The above equations are discretized assuming a fluid-type rigid-viscoplastic constitutive equation for the metal,

$$\sigma_{ij} = s_{ij} - p\delta_{ij} = 2\mu\dot{\varepsilon}_{ij} - p\delta_{ij} \,, \tag{2}$$

where $\dot{\varepsilon}_{ij} = \frac{1}{2}(\partial v_i/\partial x_j + \partial v_j/\partial x_i)$ is the rate of deformation tensor defined as the symmetric part of the velocity gradient tensor. The equivalent viscosity μ is defined as

$$\mu = \frac{\sigma_0 + (\dot{\bar{\varepsilon}}/\gamma)^{\frac{1}{n}}}{3\dot{\bar{\varepsilon}}} \,, \qquad \dot{\bar{\varepsilon}} = \sqrt{\tfrac{2}{3}\dot{\varepsilon}_{ij}\dot{\varepsilon}_{ij}} \,, \tag{3}$$

with γ (so-called fluidity) and n being parameters of the viscoplastic law, $\dot{\bar{\varepsilon}}$ the effective strain rate and σ_0 is the yield stress for the $\dot{\bar{\varepsilon}} \to 0$ limit. Assuming small changes in density, we can re-write Eqs. (1) as

$$\begin{aligned} \rho_o \frac{\partial v_i}{\partial t} &= \frac{\partial s_{ij}}{\partial x_j} - \frac{\partial p}{\partial x_i} - g_i \,, \\ \frac{1}{c^2}\frac{\partial p}{\partial t} &= -\rho_o \frac{\partial v_i}{\partial x_i} \,, \end{aligned} \tag{4}$$

where c is the speed of sound, $c^2 = K/\rho_o$, with K as the bulk modulus.

Upon discretization, Eqs. (4) yield

$$\begin{bmatrix} \mathbf{M}_{(\mathrm{v})} & \mathbf{0} \\ \mathbf{0} & \mathbf{M}_{(\rho)} \end{bmatrix} \frac{\mathrm{d}}{\mathrm{d}t} \begin{bmatrix} \mathbf{q} \\ \mathbf{p} \end{bmatrix} = - \begin{bmatrix} \mathbf{K}_{(\mu)} & \mathbf{K}_{(\mathrm{p})}^{\mathrm{T}} \\ -\mathbf{K}_{(\mathrm{p})} & \mathbf{0} \end{bmatrix} \begin{bmatrix} \mathbf{q} \\ \mathbf{p} \end{bmatrix} + \begin{bmatrix} \mathbf{Q} \\ \mathbf{0} \end{bmatrix} \tag{5}$$

where $\mathbf{q}$ and $\mathbf{p}$ are the vectors of discretized velocity and pressure, respectively. The mass matrices read

$$M_{(\mathrm{v})\alpha\beta} = \int_{\Omega} \rho_o \mathbf{N}_{(\mathrm{v})\alpha} \mathbf{N}_{(\mathrm{v})\beta} \, \mathrm{d}\Omega \,, \qquad M_{(\rho)\alpha\beta} = \int_{\Omega} \frac{1}{\rho_o c^2} \mathbf{N}_{(\mathrm{p})\alpha} \mathbf{N}_{(\mathrm{p})\beta} \, \mathrm{d}\Omega \,, \tag{6}$$

the "stiffness" matrix is formed by the submatrices

$$K_{(\mu)\alpha\beta} = \int_{\Omega} 2\mu B_{s\alpha} B_{s\beta} \, \mathrm{d}\Omega \,, \qquad K_{(p)\alpha\beta} = \int_{\Omega} 2N_{(\mathrm{p})\alpha} \Gamma_s B_{s\beta} \, \mathrm{d}\Omega \,, \tag{7}$$

and $\mathbf{Q}$ is the vector of boundary and body forces. In Eqs. (6) and 7, $\mathbf{N}_{(\mathrm{v})}$ and $\mathbf{N}_{(\mathrm{p})}$ are the shape functions for velocity and pressure, respectively, while $\mathbf{B}$ is the known strain rate-velocity matrix and $\mathbf{\Gamma} = \{1,1,1,0,0,0\}$ in 3D or $\mathbf{\Gamma} = \{1,1,0\}$ in 2D is used to obtain the volumetric strain rate.

Usually the numerical solution of the above problem requires the use of different order of interpolation for velocity and pressure to fulfill the Babuska–Brezzi condition. Alternatively, stabilization methods are available which introduce some artificial numerical parameter, (e.g. [3, 7], for direct solution methods). An equivalent effect has been obtained by time-step splitting [5, 6], with a proper choice of the split, as first noticed by Schneider [10] and Kawahara [8]. First, an intermediate velocity $\tilde{v}$ is defined such that satisfies the deviatoric part of the momentum equation (that is, dropping the pressure gradient term) for a given time step

$$\rho_o \frac{\Delta \tilde{v}_i}{\Delta t} = \frac{\rho_o}{\Delta t}(\tilde{v}_i - v_i^n) = \frac{\partial s_{ij}^n}{\partial x_j} - g_i \,. \tag{8}$$

Then, by standard explicit discretization of the time derivatives and imposing incompressibility at the end of the time step, we obtain a two-step algorithm which reads

$$\begin{aligned} &\textit{sub-step 1} \qquad \frac{1}{\Delta t}\mathbf{M}(\tilde{\bar{\mathbf{q}}} - \bar{\mathbf{q}}^n) + \mathbf{K}_1 \bar{\mathbf{q}}^n - \bar{\mathbf{Q}}^n = 0 \,, \\ &\textit{sub-step 2} \qquad \frac{1}{\Delta t}\mathbf{M}(\bar{\mathbf{q}}^{n+1} - \tilde{\bar{\mathbf{q}}}) + \mathbf{K}_2 \tilde{\bar{\mathbf{q}}} - \bar{\mathbf{Q}}_{(\mathrm{p})}^n = 0 \,, \end{aligned} \tag{9}$$

where $\bar{\mathbf{q}}$ is the vector of discretized variables (velocity and pressure), the n index indicates quantities at time t_n, and the tilde the "intermediate" quantities. In terms of velocity and pressure sub-matrices, the matrices in Eqs. (9) have the following structure,

$$\mathbf{K}_1 = \begin{bmatrix} \mathbf{K}_{(\mu)} & \mathbf{0} \\ \mathbf{0} & \mathbf{0} \end{bmatrix}; \qquad \mathbf{K}_2 = \begin{bmatrix} \mathbf{0} & \mathbf{K}_{(\mathrm{p})}^{\mathrm{T}} \\ -\mathbf{K}_{(\mathrm{p})} & \frac{\Delta t}{\rho_o}\mathbf{H} \end{bmatrix}; \qquad \mathbf{M} = \begin{bmatrix} \mathbf{M}_{(\mathrm{v})} & \mathbf{0} \\ \mathbf{0} & \mathbf{M}_{(\rho)} \end{bmatrix}, \tag{10}$$

where

$$H_{\alpha\beta} = \int_{\Omega} \frac{\partial N_{(\mathrm{p})\alpha}}{\partial x_i} \frac{\partial N_{(\mathrm{p})\beta}}{\partial x_i} \, \mathrm{d}\Omega \tag{11}$$

is the discretized Laplacian operator and $\bar{\mathbf{Q}}$ is the force vector $\mathbf{Q}$ extended by the pressure entries (which are zero) and $\bar{\mathbf{Q}}_{(\mathrm{p})}$ is a force vector which results from integrating by parts the pressure gradient term; its pressure entries read

$$Q_{(\mathrm{p})\alpha} = \frac{\Delta t}{\rho} \int_{\partial\Omega} N_{(\mathrm{p})\alpha} \frac{\partial N_{(\mathrm{p})\beta}}{\partial x_i} n_i \, \mathrm{d}(\partial\Omega) p_\beta^n \tag{12}$$

(where the vector n_i is normal to the boundary), while the velocity entries are zero. We notice that $\mathbf{K}_1 + \mathbf{K}_2$ is equal to the standard system matrix for direct solution (see Eq. (5)), except for the

pressure–pressure sub-matrix which, since it is formed by the discrete Laplacian $\mathbf{H}$, introduces a stabilizing effect upon appropriate values of $\Delta t/\rho_o$, thus allowing the use of equal order interpolations for both discretized variables.

The essential boundary conditions of the problem, corresponding to the effect of tools or forming matrices, should be applied only to the second sub-step to obtain $\bar{\mathbf{q}}^{n+1}$. The intermediate solution $\tilde{\bar{\mathbf{q}}}$ results from the first sub-step solved only with natural boundary conditions: either unloaded or loaded with imposed boundary or volume forces. To apply essential boundary conditions to calculate $\tilde{\bar{\mathbf{q}}}$ would mean that additional forces are being introduced and shoud be balanced with opposite forces in the second sub-step.

For the particular case of steady state, the system of Eqs. (9) reduces to a form only dependent on $\Delta t/\rho_o$, which meassures the amount of stabilizing effect introduced by the numerical scheme. Therefore, within the stability range, we can adjust Δt, ρ_o and c, and, if the ratio $\Delta t/\rho_o$ is kept constant, we can converge to the same solution with different convergence rates. On the other hand, ρc^2 meassures, for the transient case, the amount of artificial compressibility introduced by the method. Again, we find the group $\Delta t \rho c^2$ as characterizing the system behaviour along the time integration. Specifically, apart from measuring the accuracy with which the incompressibility condition is imposed, determines the stability of the numerical integration scheme.

3. Sensitivity expressions

The most straightforward way for sensitivity analysis of the present problem together with its numerical model is to apply the Direct Differentiation Method to the discrete set of equations. We differentiate the already discretized equilibrium equations, Eqs. (9) with respect to a design parameter h. Equivalently, we can differentiate the continuum equations and then discretize the problem, which would also include time-step splitting for the time integration of the sensitivity coefficients, although we can also assume another strategy and even another discretization for the sensitivity stage. If that is not the case, we obtain, with either method, the design-differentiated system

$$\begin{aligned}
&\frac{\partial}{\partial h}\left(\frac{1}{\Delta t}\mathbf{M}\right)(\tilde{\bar{\mathbf{q}}}-\bar{\mathbf{q}}^n)+\frac{1}{\Delta t}\mathbf{M}\left(\frac{\mathrm{d}\tilde{\bar{\mathbf{q}}}}{\mathrm{d}h}-\frac{\mathrm{d}\bar{\mathbf{q}}^n}{\mathrm{d}h}\right)+\frac{\partial \mathbf{K}_1}{\partial h}\bar{\mathbf{q}}^n+\mathbf{K}_1^t\frac{\mathrm{d}\bar{\mathbf{q}}^n}{\mathrm{d}h}-\frac{\partial \bar{\mathbf{Q}}^n}{\partial h}=0,\\
&\frac{\partial}{\partial h}\left(\frac{1}{\Delta t}\mathbf{M}\right)(\bar{\mathbf{q}}^{n+1}-\tilde{\bar{\mathbf{q}}})+\frac{1}{\Delta t}\mathbf{M}\left(\frac{\mathrm{d}\bar{\mathbf{q}}^{n+1}}{\mathrm{d}h}-\frac{\mathrm{d}\tilde{\bar{\mathbf{q}}}}{\mathrm{d}h}\right)+\frac{\partial \mathbf{K}_2}{\partial h}\tilde{\bar{\mathbf{q}}}+\mathbf{K}_2\frac{\mathrm{d}\tilde{\bar{\mathbf{q}}}}{\mathrm{d}h}-\frac{\mathrm{d}\bar{\mathbf{Q}}^n_{(\mathrm{p})}}{\mathrm{d}h}=0,
\end{aligned} \tag{13}$$

where the tangent matrix of $\mathbf{K}_1$ reads

$$\mathbf{K}_1^t=\begin{bmatrix}\mathbf{K}^t_{(\mu)} & \mathbf{0}\\ \mathbf{0} & \mathbf{0}\end{bmatrix}=\mathbf{K}_1+\begin{bmatrix}\dfrac{\partial K_{(\mu)\alpha\gamma}}{\partial q_\beta}q_\gamma & \mathbf{0}\\ \mathbf{0} & \mathbf{0}\end{bmatrix} \tag{14}$$

and the pressure entries of the derivative of $\bar{\mathbf{Q}}_{(\mathrm{p})}$ read

$$\frac{\mathrm{d}Q^n_{(\mathrm{p})\alpha}}{\mathrm{d}h}=\frac{\partial Q^n_{(\mathrm{p})\alpha}}{\partial h}+\frac{\Delta t}{\rho}\int_{\partial\Omega}N_{(\mathrm{p})\alpha}\frac{\partial N_{(\mathrm{p})\beta}}{\partial x_i}n_i\,\mathrm{d}(\partial\Omega)\frac{\mathrm{d}p^n_\beta}{\mathrm{d}h}\,. \tag{15}$$

If we obtain from Eq. (9) and replace into Eq. (13) respectively $(\tilde{\bar{\mathbf{q}}}-\bar{\mathbf{q}}^n)$ and $(\bar{\mathbf{q}}^{n+1}-\tilde{\bar{\mathbf{q}}})$, we arrive at expressions for $\mathrm{d}\tilde{\bar{\mathbf{q}}}/\mathrm{d}h$ and $\mathrm{d}\bar{\mathbf{q}}^{n+1}/\mathrm{d}h$ — our only unknowns — which do not depend, respectively, on $\tilde{\bar{\mathbf{q}}}$ and $\bar{\mathbf{q}}^{n+1}$,

$$\begin{aligned}
&\frac{\partial}{\partial h}\left(\frac{1}{\Delta t}\mathbf{M}\right)\Delta t\mathbf{M}^{-1}(\mathbf{K}_1\bar{\mathbf{q}}^n-\bar{\mathbf{Q}}^n)+\frac{1}{\Delta t}\mathbf{M}\left(\frac{\mathrm{d}\tilde{\bar{\mathbf{q}}}}{\mathrm{d}h}-\frac{\mathrm{d}\bar{\mathbf{q}}^n}{\mathrm{d}h}\right)+\frac{\partial \mathbf{K}_1}{\partial h}\bar{\mathbf{q}}^n+\mathbf{K}_1^t\frac{\mathrm{d}\bar{\mathbf{q}}^n}{\mathrm{d}h}-\frac{\partial \bar{\mathbf{Q}}^n}{\partial h}=0\,,\\
&\frac{\partial}{\partial h}\left(\frac{1}{\Delta t}\mathbf{M}\right)\Delta t\mathbf{M}^{-1}(\mathbf{K}_2\tilde{\bar{\mathbf{q}}}-\bar{\mathbf{Q}}^n_{(\mathrm{p})})+\frac{1}{\Delta t}\mathbf{M}\left(\frac{\mathrm{d}\bar{\mathbf{q}}^{n+1}}{\mathrm{d}h}-\frac{\mathrm{d}\tilde{\bar{\mathbf{q}}}}{\mathrm{d}h}\right)+\frac{\partial \mathbf{K}_2}{\partial h}\tilde{\bar{\mathbf{q}}}+\mathbf{K}_2\frac{\mathrm{d}\tilde{\bar{\mathbf{q}}}}{\mathrm{d}h}-\frac{\mathrm{d}\bar{\mathbf{Q}}^n_{(\mathrm{p})}}{\mathrm{d}h}=0\,,
\end{aligned} \tag{16}$$

therefore the sensitivity coefficients can be obtained simultaneously to them, which means that the sensitivity stage does not introduce additional steps or sub-steps, and can result simultaneous to the solution of the analysis problem.

The boundary conditions for the sensitivity stage are similar to those of the analysis stage [1, 12]: only natural for the intermediate quantities ($\mathrm{d}\tilde{\bar{\mathbf{q}}}/\mathrm{d}h$), and essential and natural for the end-of-step quantities ($\mathrm{d}\bar{\mathbf{q}}^{n+1}/\mathrm{d}h$), according to the imposed geometrical restrictions. It should be noticed that to boundaries with non-zero imposed values corresponds zero sensitivity.

The design parameter h can be any material, shape and numerical parameter (as the time step), which means that sensitivity analysis may be used to asses the effect of assuming certain values of them. For shape sensitivity analysis (which is not covered in this paper) the above formalism should be used in conjunction with the respective available methods (i.e. Domain parametrization and Material derivative approachs). Within direct solution methods such techniques have been applied to metal forming in [9].

4. Numerical illustrations

4.1. Steady state extrusion

First, a steady state extrusion process is simulated. The layout and finite element mesh are shown in Fig. 1. Velocities are imposed on the left side thus simulating the effect of the ram. Boundary friction is simulated using contact elements that impose a Coulomb friction force proportional to the pressure, with a velocity restriction to avoid oscillations around sticking friction. Time integration is carried out with a fixed mesh until steady state is achieved. Figure 2 shows the velocity module and pressure surfaces as seen from the upper right corner of the extrusion matrix. The velocity grows smoothly from 1 to 4, according to the extrusion ratio. The pressure shows compression inside the die and an unloading towards the exit with a slight oscillation due to the effect of boundary conditions near the outlet. Figures 3 to 5 show the sensitivity of both quantities with respect to the parameters of the constitutive equation: yield stress σ_0, fluidity γ and index of the viscoplastic law n, respectively. The assumed values for these quantities are: $\sigma_0 = 200$, $\gamma = 10^{-6}$ and $n = 1.5$, corresponding to a rather rate sensitive material as steel in hot working conditions. In every case the

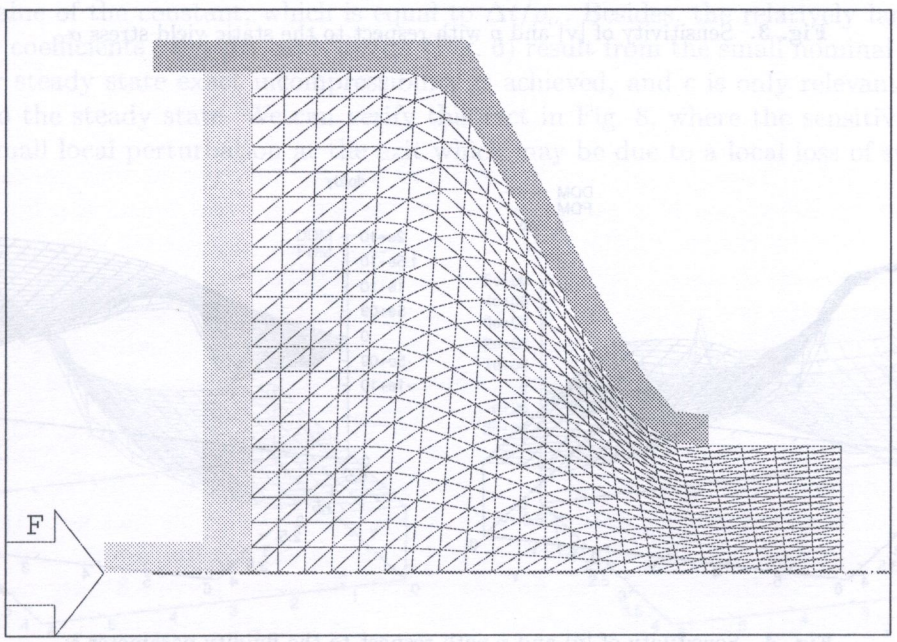

Fig. 1. Layout of the extrusion process

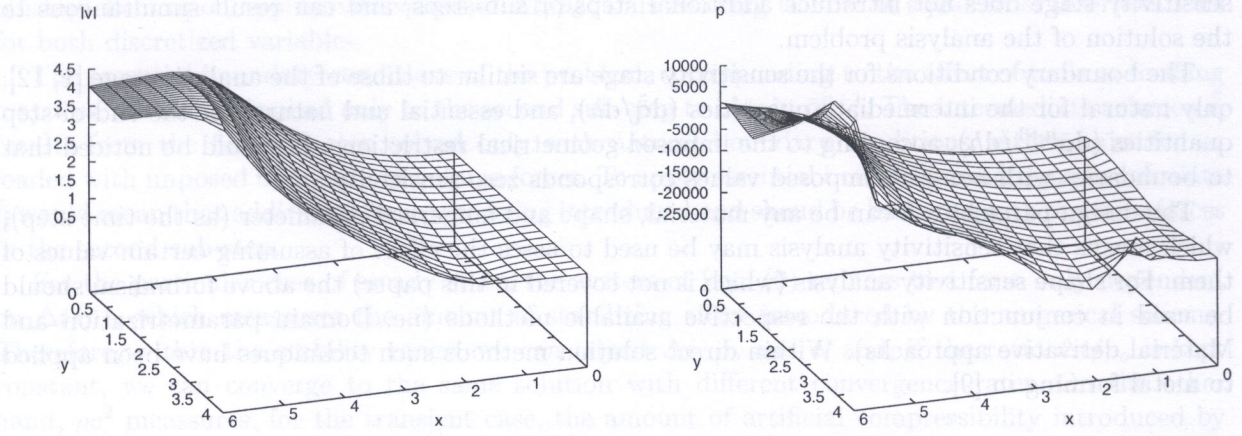

Fig. 2. Velocity module $|\mathbf{v}|$ and pressure p

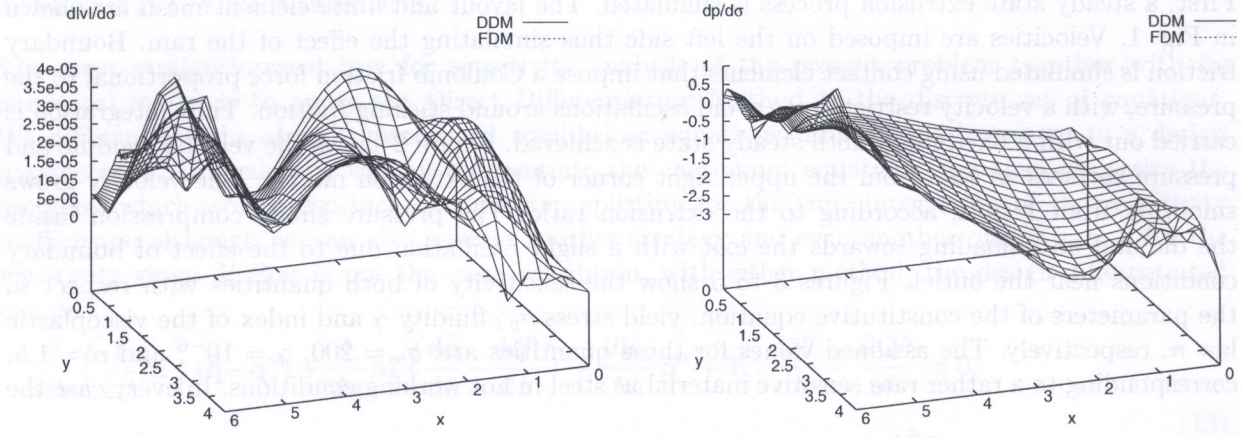

Fig. 3. Sensitivity of $|\mathbf{v}|$ and p with respect to the static yield stress σ

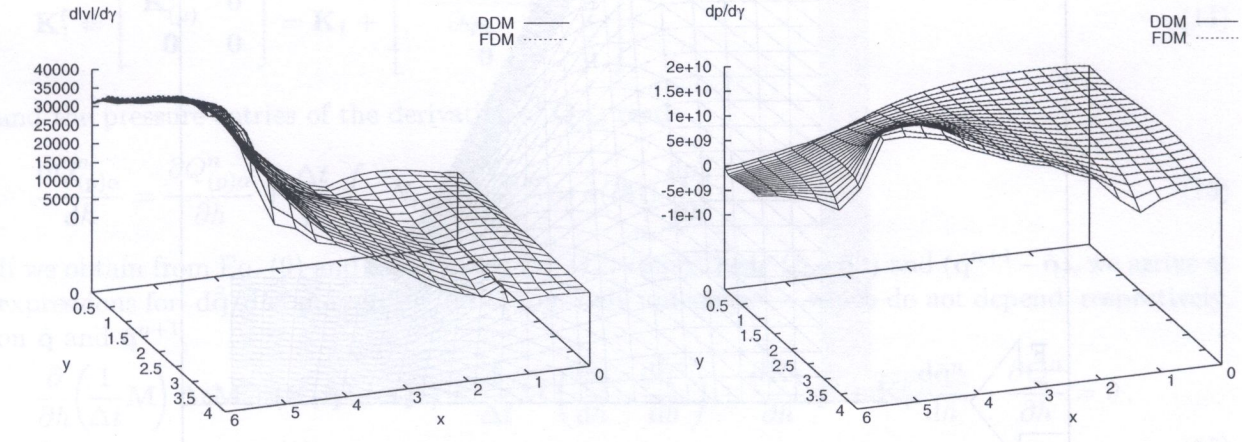

Fig. 4. Sensitivity of $|\mathbf{v}|$ and p with respect to the fluidity parameter γ

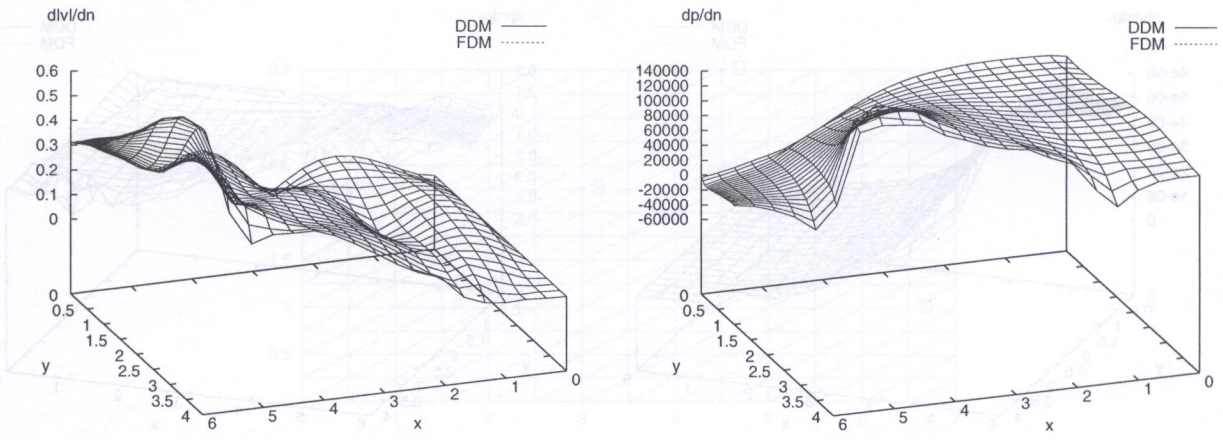

Fig. 5. Sensitivity of $|\mathbf{v}|$ and p with respect to the viscoplastic index n

DDM and FDM solutions are in good agreement, either when the sensitivity coefficients are small with respect to the values of the variable (Fig. 3a) or very large (Fig. 4b) The characteristics of these results are the same as for the solution by a direct method, as has been presented in [3]: for this case of imposed velocities (instead of imposed boundary force) the pressure sensitivity with respect to the yield stress is quite proportional to the pressure itself, and the velocity module is almost insensitive. Results are very sensitive to the fluidity, which is in agreement with its small nominal value. Velocity sensitivities grow from zero in contact with the ram (where velocity is imposed) to its maximal value at the exit. Conversely, pressure sensitivities are at their maximum near the ram and drop to zero at the exit.

Sensitivity analysis can also be applied to obtain information about the numerical method used to simulate a given process [2]. In particular, in the present example the time step Δt, the material density ρ_o and the sound velocity c have been taken as design parameters for nominal values of 10^{-6}, 10, and 10^{-11}, respectively. The sensitivities of the velocity module and pressure with respect to them are shown in Figs. 6 to 8. Again, agreement is found between FDM and DDM. We can see that sensitivities with respect to material density are proportional to those with respect to the time step, with a negative proportionality constant for the pressure. From Figs. 6 and 7 we can get 10^{-7} as the value of the constant, which is equal to $\Delta t/\rho_o$. Besides, the relatively large values for the sensitivity coefficients $\mathrm{d}|v|/\mathrm{d}h$ and $\mathrm{d}p/\mathrm{d}h$ (Fig. 6) result from the small nominal values of the time step. For steady state exact incompressibility is achieved, and c is only relevant for speed of convergence to the steady state. We can verify this fact in Fig. 8, where the sensitivities are zero except for a small local perturbation at the exit which may be due to a local loss of stability.

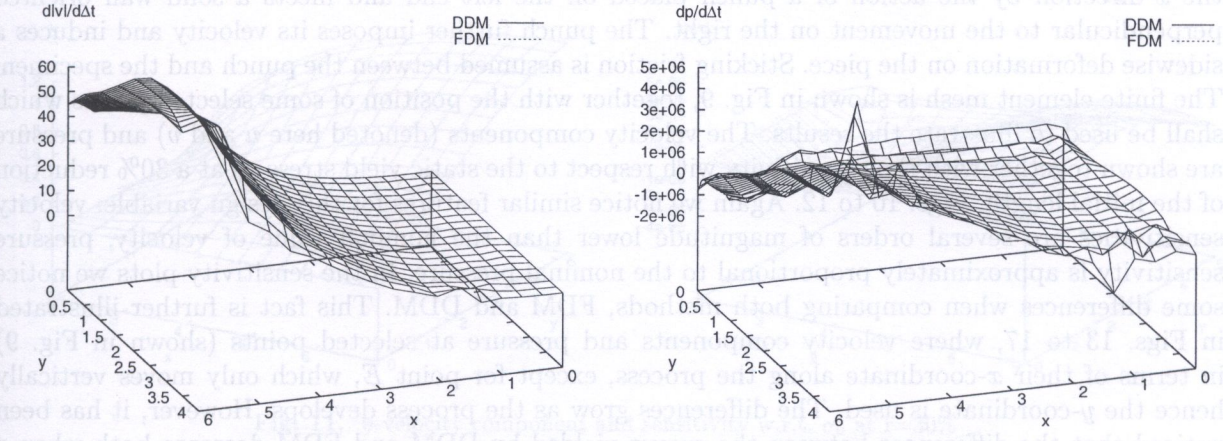

Fig. 6. Sensitivity of $|\mathbf{v}|$ and p with respect to the time step size Δt

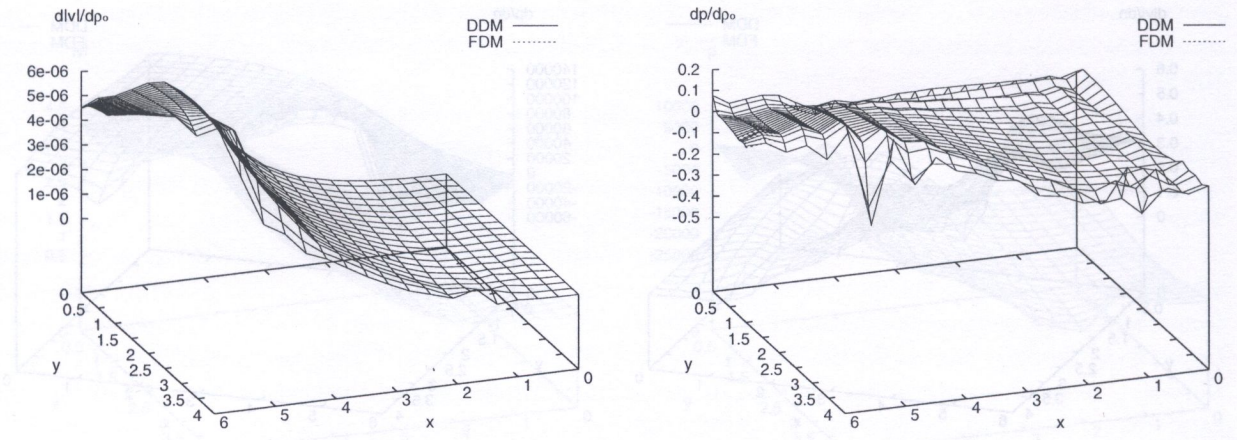

Fig. 7. Sensitivity of $|\mathbf{v}|$ and p with respect to the density ρ_o

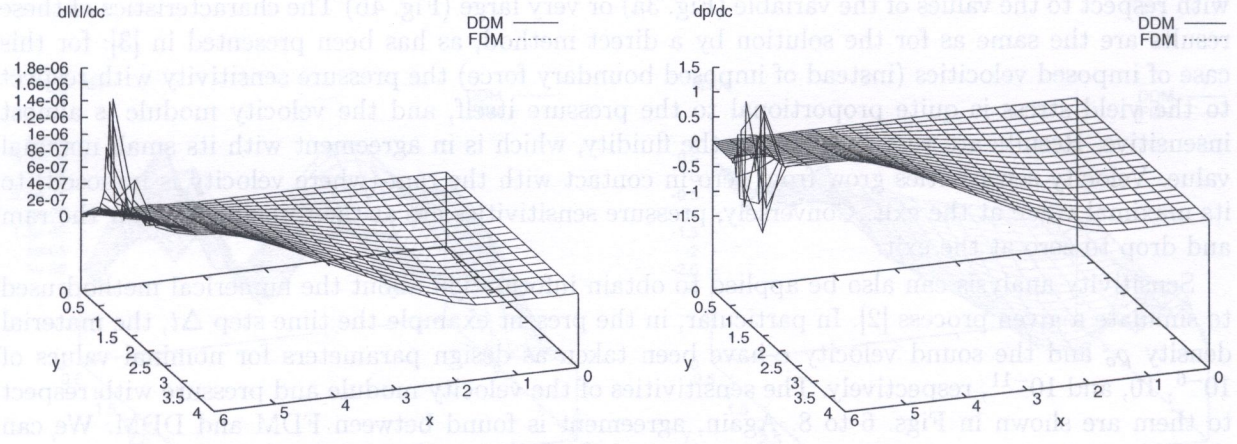

Fig. 8. Sensitivity of $|\mathbf{v}|$ and p with respect to the velocity c

4.2. Upsetting

In the next example a transient process is simulated. An initially rectangular specimen moves in the x-direction by the action of a punch placed on the left end and meets a solid wall oriented perpendicular to the movement on the right. The punch further imposes its velocity and induces a sidewise deformation on the piece. Sticking friction is assumed between the punch and the specimen. The finite element mesh is shown in Fig. 9, together with the position of some selected points which shall be used to illustrate the results. The velocity components (denoted here u and v) and pressure are shown together with their sensitivity with respect to the static yield stress σ_0 at a 30% reduction of the initial length, Figs. 10 to 12. Again we notice similar features for this design variable: velocity sensitivities are several orders of magnitude lower than the nominal value of velocity, pressure sensitivity is approximately proportional to the nominal pressure. In the sensitivity plots we notice some differences when comparing both methods, FDM and DDM. This fact is further illustrated in Figs. 13 to 17, where velocity components and pressure at selected points (shown in Fig. 9) in terms of their x-coordinate along the process, except for point E, which only moves vertically hence the y-coordinate is used. The differences grow as the process develops. However, it has been noticed that the differences between the curves yielded by DDM and FDM decrease both when a smaller perturbation is taken and when the time step size Δt is reduced. These facts highlight the

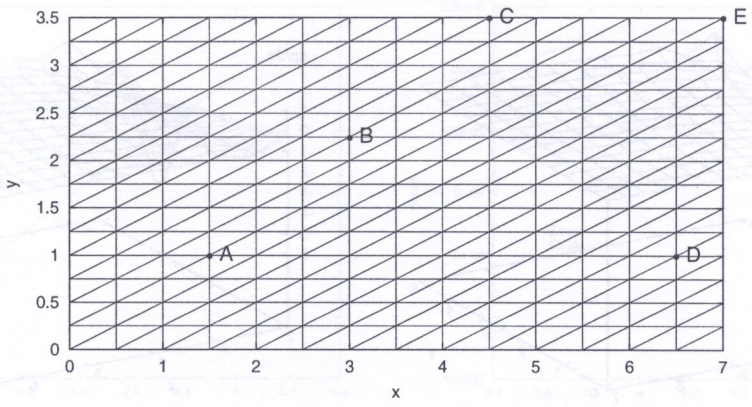

Fig. 9. Upsetting: initial mesh and selected points

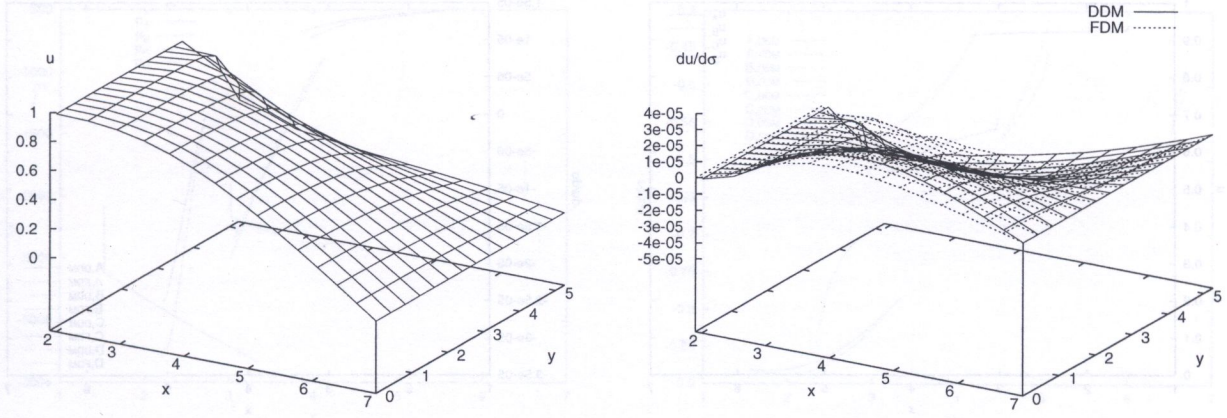

Fig. 10. x-velocity component and sensitivity w.r.t. σ_0 at r=30%

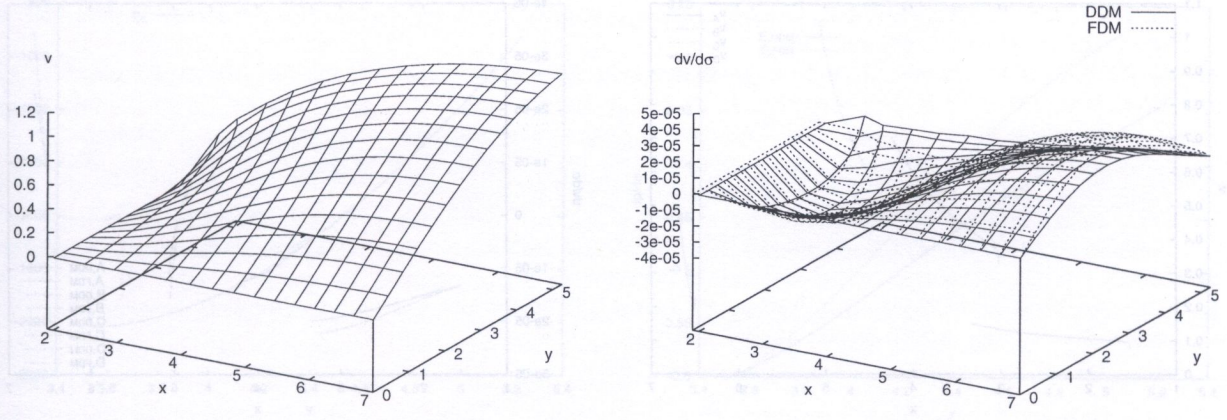

Fig. 11. y-velocity component and sensitivity w.r.t. σ_0 at r=30%

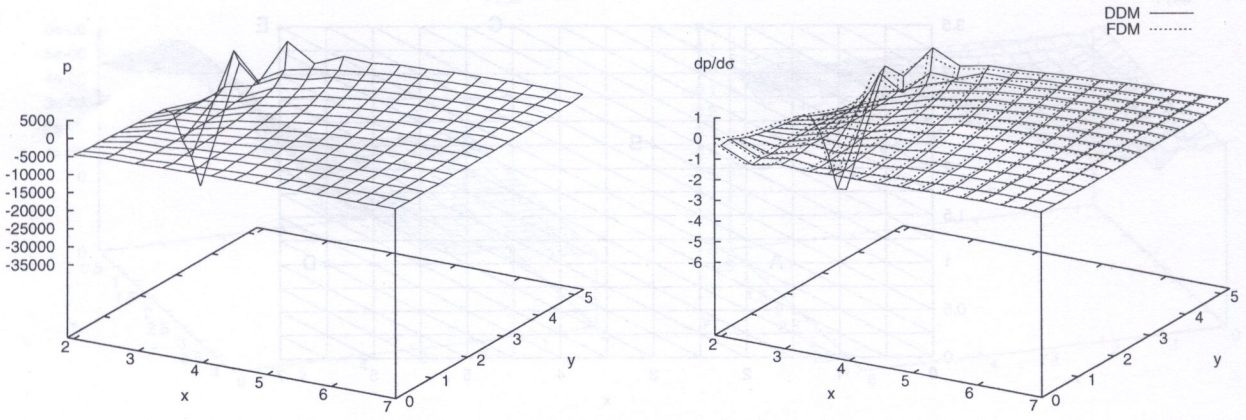

Fig. 12. Pressure and sensitivity w.r.t. σ_0 at r=30%

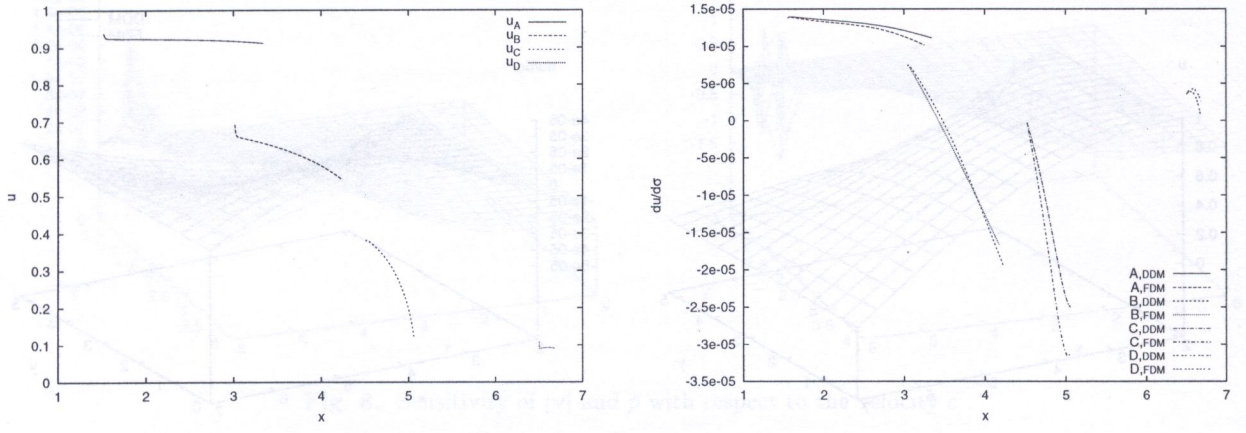

Fig. 13. x-velocity component and sensitivity w.r.t. σ_0 *vs* x-coordinate

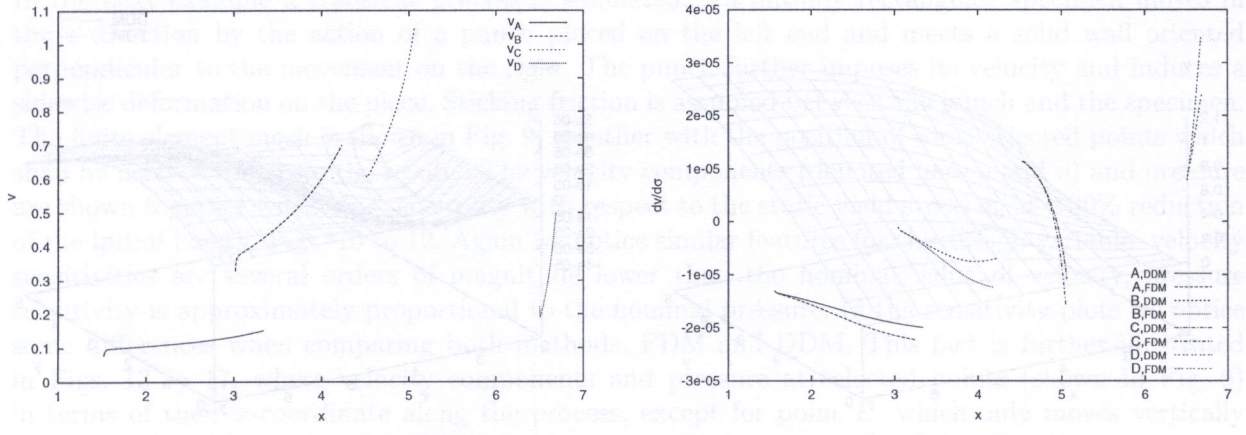

Fig. 14. y-velocity component and sensitivity w.r.t. σ_0 *vs* x-coordinate

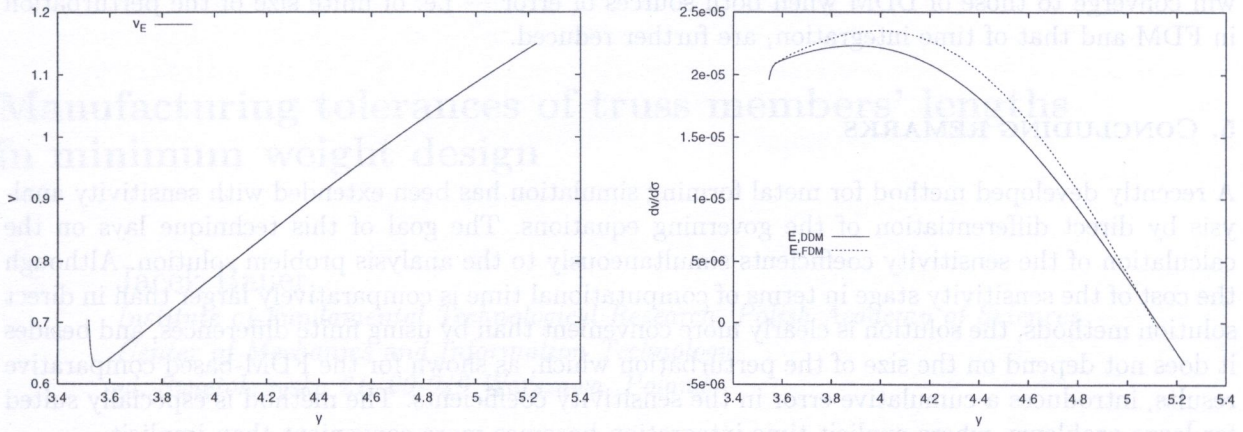

Fig. 15. y-velocity component and sensitivity w.r.t. σ_0 *vs* y-coordinate

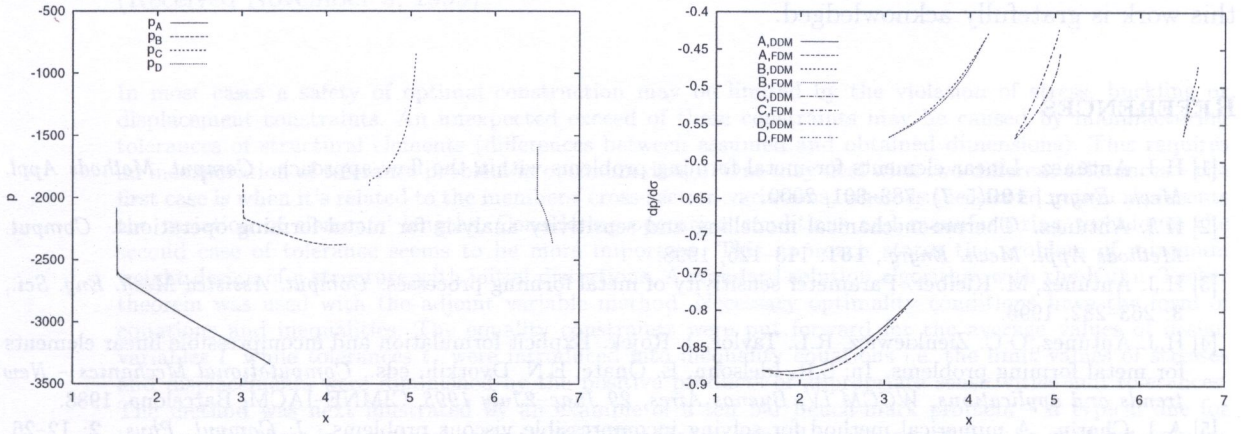

Fig. 16. Pressure and sensitivity w.r.t. σ_0 *vs* x-coordinate

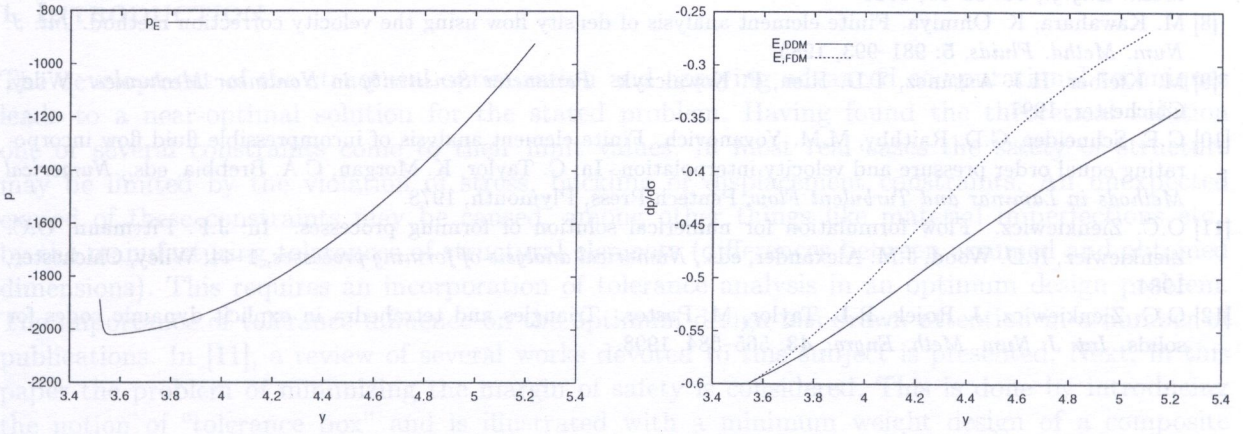

Fig. 17. Pressure and sensitivity w.r.t. σ_0 *vs* y-coordinate

cummulative nature of the error, characteristic of explicit methods, and suggests that FDM results will converge to those of DDM when both sources of error — i.e. of finite size of the perturbation in FDM and that of time integration, are further reduced.

5. Concluding remarks

A recently developed method for metal forming simulation has been extended with sensitivity analysis by direct differentiation of the governing equations. The goal of this technique lays on the calculation of the sensitivity coefficients simultaneously to the analysis problem solution. Although the cost of the sensitivity stage in terms of computational time is comparatively larger than in direct solution methods, the solution is clearly more convenient than by using finite differences, and besides it does not depend on the size of the perturbation which, as shown for the FDM-based comparative results, introduces a cumulative error in the sensitivity coefficients. The method is especially suited for large problems, where explicit time integration becomes more convenient than implicit.

6. Acknowledgements

The financial support of the Polish Scientific Committee under grant no. T811F01512 for part of this work is gratefully acknowledged.

References

[1] H.J. Antúnez. Linear elements for metal forming problems within the flow approach. *Comput. Methods Appl. Mech. Engrg.*, **190**(5–7): 783–801, 2000.

[2] H.J. Antúnez. Thermo-mechanical modelling and sensitivity analysis for metal-forming operations. *Comput. Methods Appl. Mech. Engrg.*, **161**: 113–125, 1998.

[3] H.J. Antúnez, M. Kleiber. Parameter sensitivity of metal forming processes. *Comput. Assisted Mech. Eng. Sci.*, **3**: 263–282, 1996.

[4] H.J. Antúnez, O.C. Zienkiewicz, R.L. Taylor, J. Rojek. Explicit formulation and incompressible linear elements for metal forming problems. In: S.R. Idelsohn, E. Onate, E.N. Dvorkin, eds., *Computational Mechanics - New trends and applications, WCCM IV, Buenos Aires, 29 June–2July 1998*, CIMNE–IACM, Barcelona, 1988.

[5] A.J. Chorin. A numerical method for solving incompressible viscous problems. *J. Comput. Phys.*, **2**: 12–26, 1967.

[6] A.J. Chorin. On the convergence of discrete approximation to the Navier–Stokes equations. *Math. Comput.*, **23**, 1969.

[7] T.J.R. Hughes, L.P. Franca, M. Ballestra. Circumventing the Babuska–Brezzi conditions, a stable Petrov–Galerkin formulation of the stokes problem accommodating equal-order interpolation. *Comput. Methods Appl. Mech. Engrg.*, **59**: 85–99, 1986.

[8] M. Kawahara, K. Ohmiya. Finite element analysis of density flow using the velocity correction method. *Int. J. Num. Methd. Fluids*, **5**: 981–993, 1985.

[9] M. Kleiber, H.J. Antúnez, T.D. Hien, P. Kowalczyk. *Parameter Sensitivity in Nonlinear Mechanics.* Wiley, Chichester, 1997.

[10] G.E. Schneider, G.D. Raithby, M.M. Yovanovich. Finite element analysis of incompressible fluid flow incorporating equal order pressure and velocity interpolation. In: C. Taylor, K. Morgan, C.A. Brebbia, eds., *Numerical Methods in Laminar and Turbulent Flow*, Pentech Press, Plymouth, 1978.

[11] O.C. Zienkiewicz. Flow formulation for numerical solution of forming processes. In: J.F. Pittmann, O.C. Zienkiewicz, R.D. Wood, J.M. Alexander, eds., *Numerical analysis of forming processes*, 1–44, Wiley, Chichester, 1984.

[12] O.C. Zienkiewicz, J. Rojek, R.L. Taylor, M. Pastor. Triangles and tetrahedra in explicit dynamic codes for solids. *Int. J. Num. Meth. Engrg.*, **43**: 565–584, 1998.